Supplemental Information

Unsupervised discovery of behaviorally

relevant brain states in rats

playing hide-and-seek

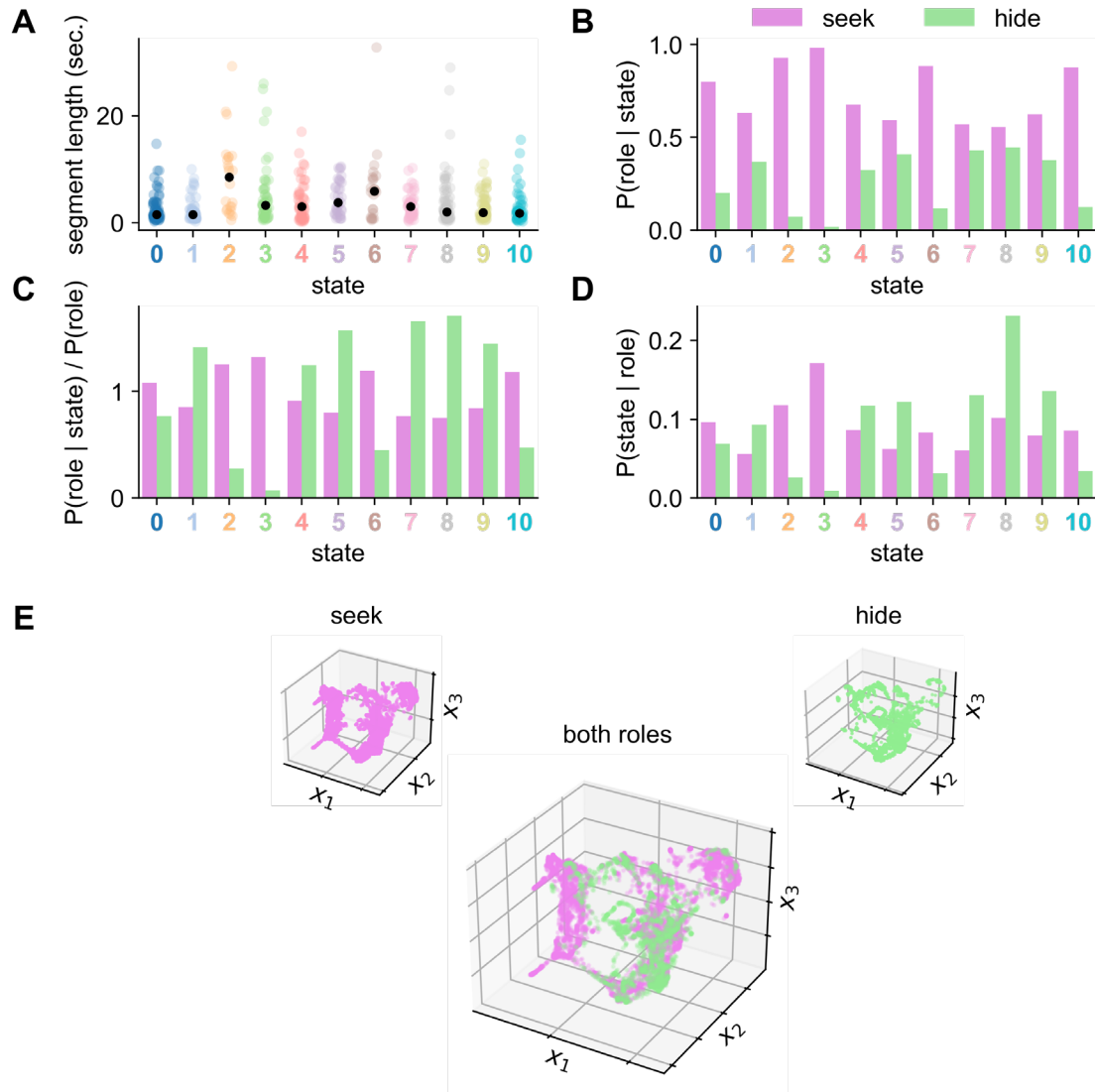Bence Bagi, Michael Brecht, and Juan Ignacio Sanguinetti-Scheck

Figure S1) State segment lengths and state usage in the hide-and-seek roles in the reference session. Related to Figure 2. A) Segment lengths for each HMM state. Median values indicated in black. **B)** P(role | state) **C)** P(role | state) / P(role). This normalization takes into account that seek trials are longer and hence more probable. **D)** P(state | role) **E)** UMAP embeddings of neural activity colored by hide-and-seek role.
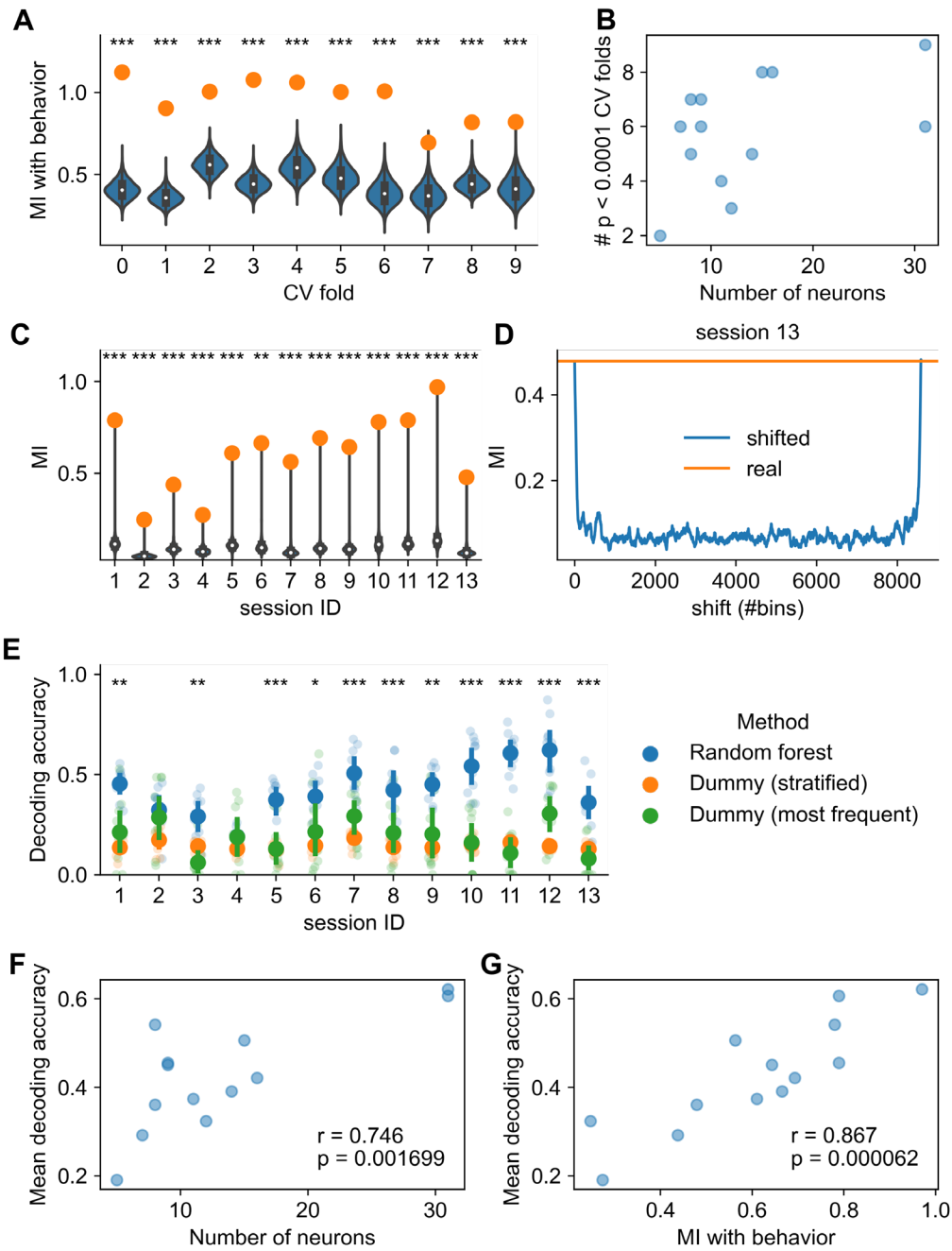
Figure S2) Cross-validated mutual information analysis and supervised decoding of behavioral states. **Related to Figure 2. A)** Fitting an HMM on a subset of trials, then applying on held-out

trials and performing the same shuffling analysis as in Fig 2E on the reference session. The star-code shows the p-value for the bootstrap with *=0.05, **=0.01, ***=0.001 **B)** Number of significant cross-validation folds (out of 10 folds) per session as a function of the number of recorded neurons in that session (using $p < 0.0001$, as this level was found to be true for every session without cross-validation in Fig 2E). **C)** Mutual information of HMM states vs behavior analysis (orange dot) for all sessions compared to a circular shuffling of the HMM states by all possible time-shifts (blue distribution) **D)** Figure shows for session #12 how the consecutive shifts affect mutual information. **E)** Cross-validated decoding of behavioral states from GPFA factors (10-fold CV across trials) using a random-forest classifier performs better than chance (performance of dummy classifiers) (one-sided Wilcoxon signed-rank test). The star-code shows the p-value with *=0.05, **=0.01, ***=0.001 **F)** Mean decoding accuracy increases with the number of neurons. (Pearson correlation, one-sided test). **G)** Mean decoding accuracy increases with the MI with behavior on the same session. (Pearson correlation, one-sided test.)
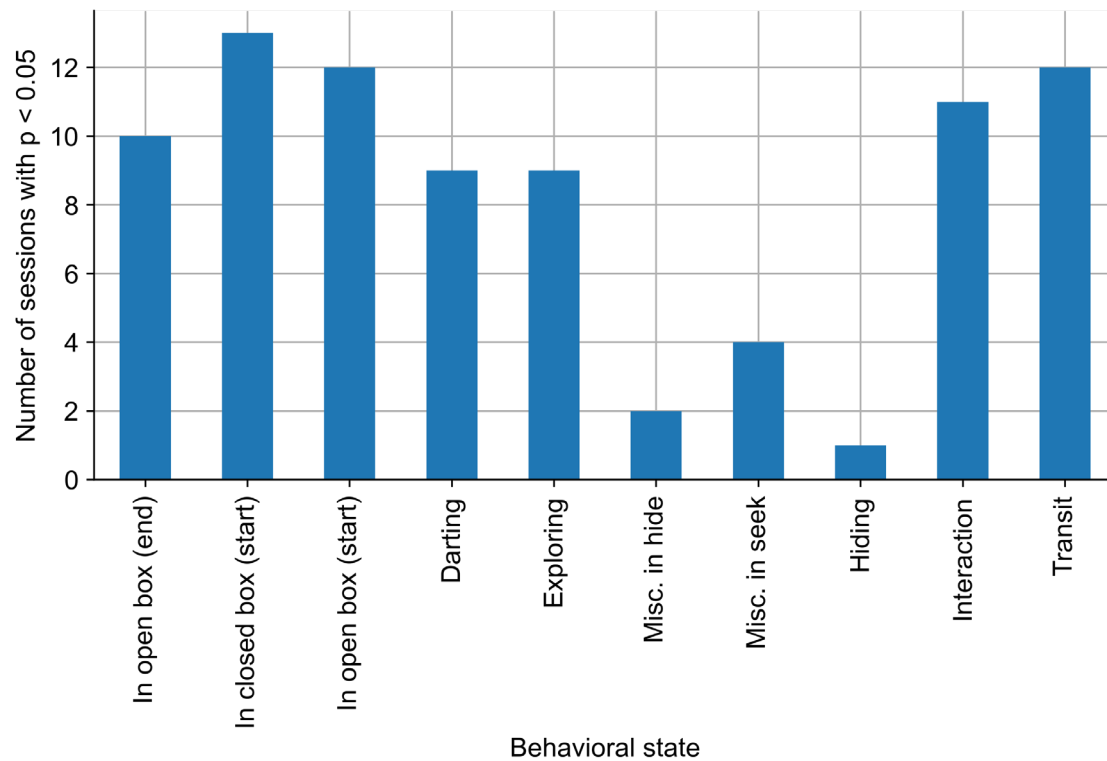
Figure S3) Significant sessions per behavior. Related to Figure 3. The number of sessions (out of 13) in which there is an HMM state significantly correlated with a tagged behavioral state ($p < 0.05$, Holm-Bonferroni correction for multiple comparisons)
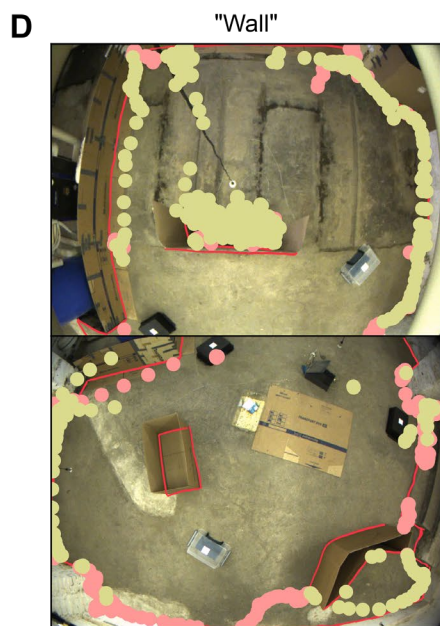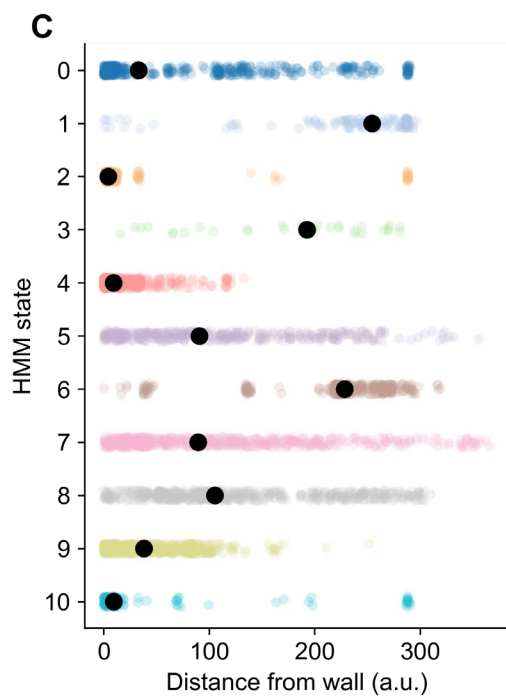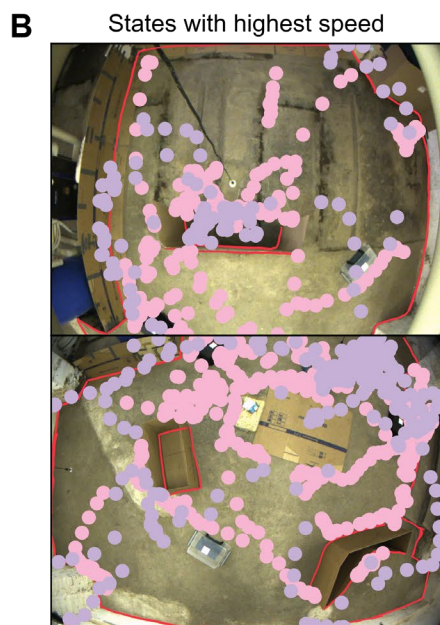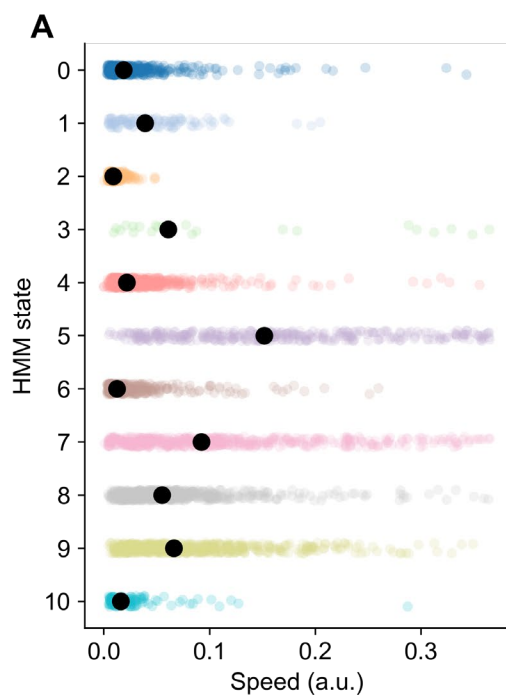
A

B States with highest speed

C

D "Wall"

Figure S4) Quantification of the "wall" and "running" states. Related to Figure 4. A) Animal's approximate speed when each state was active. One data point per timestep. **B)** Animal's position when states #7 (running) and #5 (transit) were active. **C)** Animal's approximate distance from the nearest wall when each state was active. **D)** Animal's positions when states #9 and #4 were active. These states were active when the animal was walking along (#9 and #4) and stopping at (#4) walls.
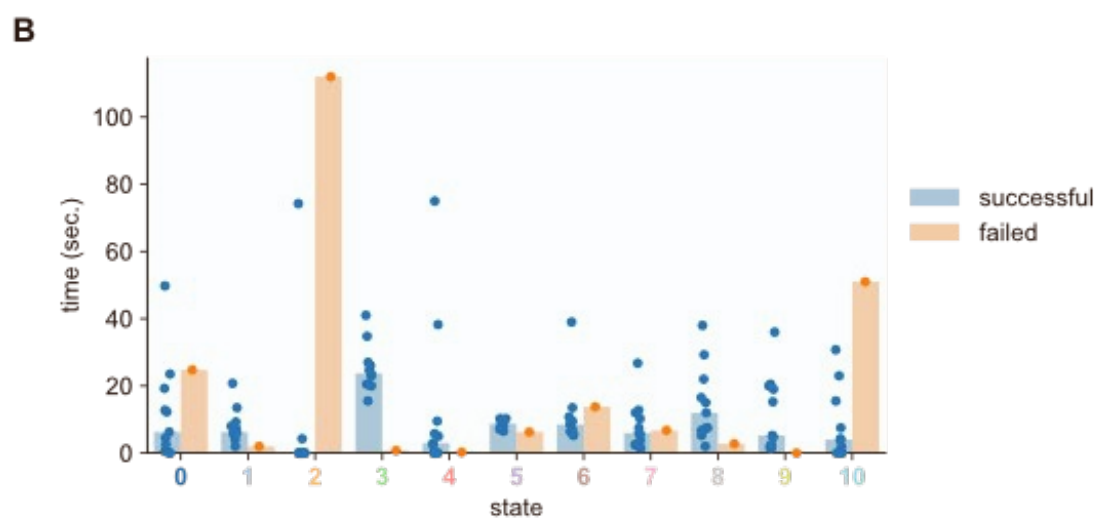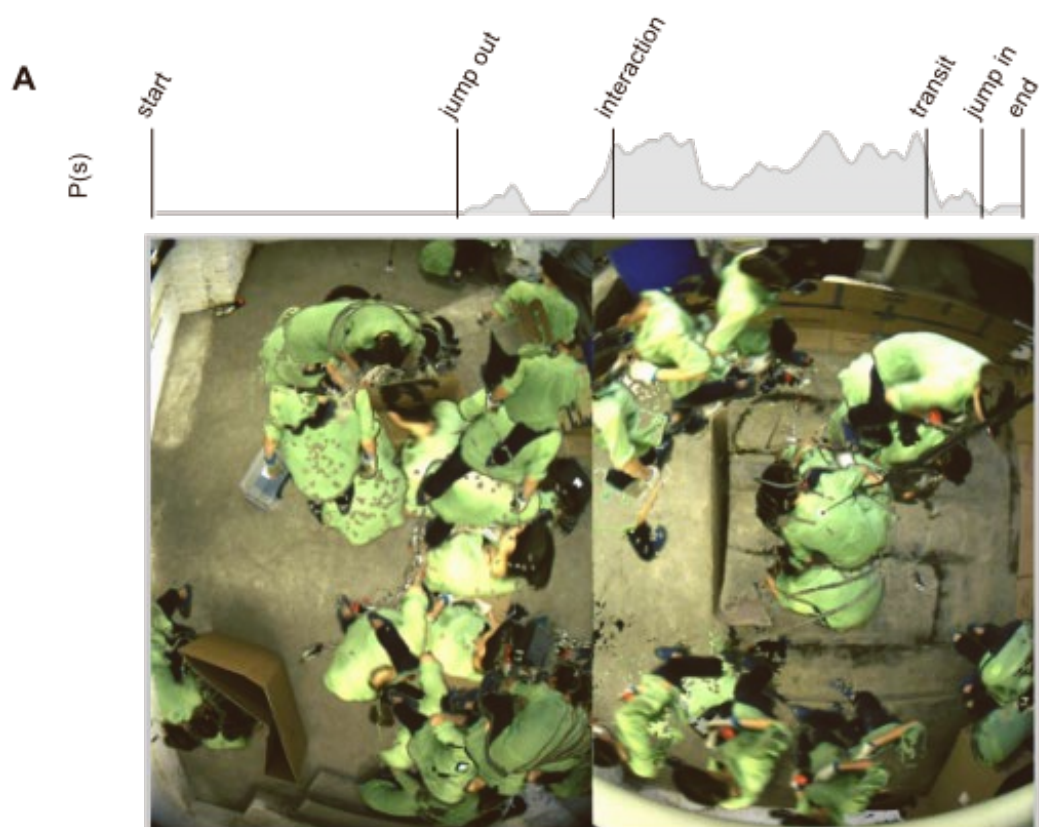
A

B

Figure S5) Interaction-related state and its absence in failed trials. Related to Figure 4. A) Condensed video frames during state #8 show interaction with the experimenter. Marginal: probability of the state #8 throughout the trial, averaged across all trials of the reference session. **B)** Time spent in the different states for the reference session on failed and successful trials of seek behavior. Note that for successful trials state #8 (playing with the experimenter) has significantly longer durations than for the single failed seek trial. Note that the failed trial is dominated by states #2 and #10 that we have post-hoc discovered as resting states.
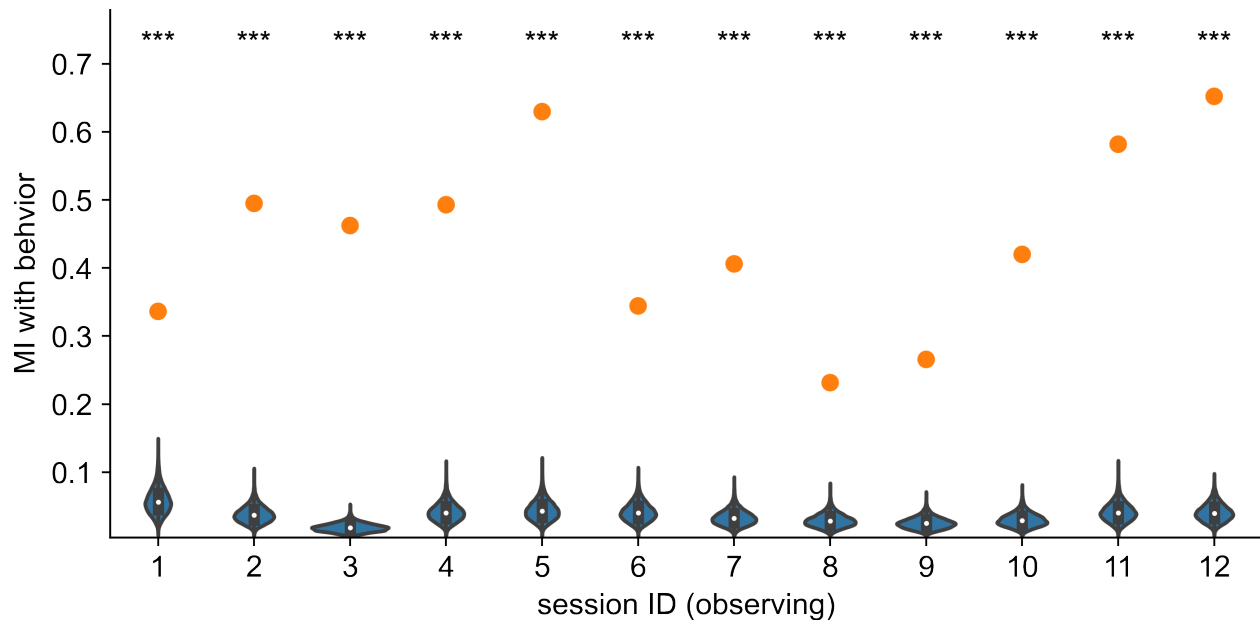
Figure S6) Separation between playing and observing. Related to Figure 6. The separation between playing- and observing states, quantified by mutual information, is well above chance level (p < 0.0001 in all sessions). The star-code shows the p-value for the bootstrap with *=0.05, **=0.01, ***=0.001